

How to Report Record Open-Circuit Voltages in Lead-Halide Perovskite Solar Cells

Lisa Krückemeier,* Uwe Rau, Martin Stolterfoht, and Thomas Kirchartz*

Open-circuit voltages of lead-halide perovskite solar cells are improving rapidly and are approaching the thermodynamic limit. Since many different perovskite compositions with different bandgap energies are actively being investigated, it is not straightforward to compare the open-circuit voltages between these devices as long as a consistent method of referencing is missing. For the purpose of comparing open-circuit voltages and identifying outstanding values, it is imperative to use a unique, generally accepted way of calculating the thermodynamic limit, which is currently not the case. Here a meta-analysis of methods to determine the bandgap and a radiative limit for open-circuit voltage is presented. The differences between the methods are analyzed and an easily applicable approach based on the solar cell quantum efficiency as a general reference is proposed.

1. Introduction

The efficient conversion of solar radiation into electrical power by a solar cell requires absorbing the photons, creating charge carriers, collecting them at the junction and finally doing so at a nonzero free energy per extracted charge carrier.^[1–3] In order to compare the ability of a solar cell to generate a high free energy per charge carrier inside its absorber—as the origin of a high photovoltage—the solar cell is held at open circuit and the voltage under one-sun illumination is measured. Comparison of open-circuit voltages in classical solar cell technologies with a fixed bandgap like crystalline Si is straightforward: the higher the better. However, once the bandgap changes within a family of materials, higher is not necessarily better anymore,

because the point of reference changes with bandgap energy.^[4] In crystalline semiconductors, bandgap is a well-defined concept as long as aspects such as structure, stoichiometry, temperature, and pressure are kept constant. However, also in crystalline materials the determination of bandgap from an actual device may not be straightforward (for instance because stoichiometry and bandgap change with depth,^[5] such as in most high efficiency chalcopyrite solar cells). In amorphous^[6] or molecular semiconductors, the whole concept of “bandgap” would not be well defined anymore and various different ways of deriving a “bandgap” from experi-


mental data coexist. In particular in organic solar cells, the topic of comparing open-circuit voltages and referencing those to different definitions of bandgap has therefore been the subject of several recent publications.^[7–9]

In the case of the emerging technology of lead-halide perovskites, the challenge of defining a bandgap initially seems less severe. The absorption edge of lead-halide perovskites is relatively sharp^[10] and there is little subgap absorption smearing out the absorption onset or the quantum efficiency spectrum. However, bandgaps in lead-halide perovskites change over a considerable range depending on the exact composition of the perovskite,^[11] making it difficult to compare, e.g., the open-circuit voltages between devices without having a consistent method of referencing. As will be shown in the present paper, there is a multitude of bandgap definitions (i.e., procedures to derive a bandgap from experimental data) used in the perovskite community. These methods lead to bandgap energies that may differ by 80 meV for one and the same device. Often,^[12–15] these bandgap energies are used to compare the device performance with the limiting situation given by the Shockley–Queisser (SQ) model.^[16] This is especially critical in case of open-circuit voltages, which in many of the compositions of lead-halide perovskites approach the radiative limit to within a few units of the thermal energy kT ,^[12,13,17] implying that already small uncertainties in the determination of the bandgap and in the subsequent calculation of the limiting open-circuit voltage may corrupt any quantitative difference between the actually measured value and the limiting one.

Here, we compare the different definitions of bandgap used in the literature and show how the thermodynamic limit to the open-circuit voltage based on the Shockley–Queisser model^[16] varies widely depending on the definition used. Therefore, referencing the open-circuit voltage of an actual device to the SQ

L. Krückemeier, Prof. U. Rau, Prof. T. Kirchartz
IEK5-Photovoltaics
Forschungszentrum Jülich
52425 Jülich, Germany
E-mail: l.krueckemeier@fz-juelich.de; t.kirchartz@fz-juelich.de

Dr. M. Stolterfoht
Institute of Physics and Astronomy
University of Potsdam
Karl-Liebknecht-Str. 24-25, D-14476 Potsdam-Golm, Germany
Prof. T. Kirchartz
Faculty of Engineering and CENIDE
University of Duisburg-Essen
Carl-Benz-Str. 199, 47057 Duisburg, Germany

 The ORCID identification number(s) for the author(s) of this article can be found under <https://doi.org/10.1002/aenm.201902573>.

© 2019 The Authors. Published by WILEY-VCH Verlag GmbH & Co. KGaA, Weinheim. This is an open access article under the terms of the Creative Commons Attribution License, which permits use, distribution and reproduction in any medium, provided the original work is properly cited.

DOI: 10.1002/aenm.201902573

case is subject to a large uncertainty introduced by the choice of the bandgap. We then compare these open-circuit voltages with the so-called radiative open-circuit voltage^[18] that can be derived from the measured absorption and electroluminescence spectra. We find that thanks to the sharp band edge and the small variations in Urbach tail slope, the radiative open-circuit voltage can always be determined for perovskite solar cells as long as an external photovoltaic quantum efficiency is available for a specific device. Therefore a meta-analysis of previously published perovskite solar cells with high open-circuit voltages (relative to the bandgap) becomes possible where all devices are compared using an identical way of referencing the open-circuit voltages to their radiative limit. Finally, we provide an outlook showing how all aspects of photovoltaic device efficiency, i.e., losses in absorption and charge collection, recombination losses and resistive losses can all be referenced and compared in a self-consistent way. We find that if current high-efficiency perovskite solar cells are compared with state-of-the-art devices from other photovoltaic technologies, their resistive losses stand out as providing the highest potential for further improvement.

2. Thermodynamics of the Open-Circuit Voltage

The SQ model defines the maximum power-conversion efficiency of a solar cell consisting of a semiconducting absorber with a single bandgap E_g^{SQ} , using the basic thermodynamic principle of detailed balance.^[16] The SQ model is however an idealized approach in which the solar cell is characterized by ideal extraction and absorption properties (see also ref. [19]). Assuming that the quantum efficiency $Q_e^{PV}(E)$ equals the absorptance $a(E)$, which behaves as a function of energy E like a step-function, the solar cell is defined only by its bandgap energy E_g^{SQ} , and its temperature T . Although this simplification is elegant and intuitive, no real semiconductor material could ever have an infinitely sharp absorption edge. Therefore, there is always a discrepancy between the calculated SQ efficiency, η^{SQ} , and the actual thermodynamic efficiency limit of a real-world solar cell with realistic absorption properties.^[4,20,21] In addition, if experimental data is compared to the SQ efficiency for a certain bandgap, the chosen definition of the bandgap^[4] affects the calculated SQ efficiency and the corresponding limit of open-circuit voltage.

Adapting the general idea of the SQ model to real devices with nonstep-function-like absorptances or quantum efficiencies leads us to a definition of the radiative limit.^[21–23] As its name implies, it is assumed, just as in the SQ situation, that all recombination processes occur radiatively. In this case, the solar cell is then explicitly defined only by its quantum efficiency and its temperature. Using these parameters in the framework of detailed balance enables us to derive a general expression for the short-circuit current density

$$J_{sc} = q \int_0^{\infty} Q_e^{PV}(E) \phi_{sun}(E) dE \quad (1)$$

where q is the elementary charge and $\phi_{sun}(E)$ is the solar spectrum. The radiative saturation-current density is



Lisa Krückemeier is a doctoral candidate in the organic and hybrid solar cells group at the Research Centre Jülich (Institute for Energy and Climate Research). She completed her Master's degree in NanoEngineering at the University Duisburg-Essen, specializing in Nanoelectronics and Nano-Optoelectronics. Her

research focuses on the understanding of loss-mechanisms in solar cells, especially losses at interfaces, and device physics of perovskite solar by combining electrical and optoelectronic characterization methods und device simulations.



Uwe Rau is currently director of the Institute for Energy and Climate Research-5 (Photovoltaics) at Research Centre Jülich. He is also professor at RWTH Aachen, Faculty of Electrical Engineering and Information Technology where he holds the Chair of Photovoltaics. Previously, he was senior researcher

at the University Stuttgart as well as post-doc at the University Bayreuth and at the Max-Planck-Institute for Solid State Research in Stuttgart. His research interest covers electronic and optical properties of semiconductors and semiconductor devices, especially characterization, simulation, and technology of solar cells and solar modules.



Thomas Kirchartz is currently a professor of electrical engineering and information technology at the University Duisburg-Essen and the head of the Department of Analytics and Simulation and the group of organic and hybrid solar cells at the Research Centre Jülich (Institute for Energy and Climate Research).

Previously, he was a Junior Research Fellow at Imperial College London. His research interests include all aspects regarding the fundamental understanding of photovoltaic devices including their characterization and simulation.

derived using the optoelectronic reciprocity^[24] and is calculated via^[18]

$$J_0^{\text{rad}} = q \int_0^\infty Q_e^{\text{PV}}(E) \phi_{\text{bb}}(E) dE \quad (2)$$

where

$$\phi_{\text{bb}}(E) = \frac{2\pi E^2}{h^3 c^2} \frac{1}{\left[\exp(E/kT) - 1 \right]} \approx \frac{2\pi E^2}{h^3 c^2} \exp\left(\frac{-E}{kT}\right) \quad (3)$$

is the blackbody spectrum at temperature T (of the solar cell), h is Planck's constant, k Boltzmann's constant, and c denotes the speed of light in vacuum. Finally, we calculate the radiative limit for the open-circuit voltage $V_{\text{oc}}^{\text{rad}}$ via^[24]

$$V_{\text{oc}}^{\text{rad}} = \frac{kT}{q} \ln\left(\frac{J_{\text{sc}}}{J_0^{\text{rad}}} + 1\right) \quad (4)$$

Note that the radiative open-circuit voltage defined by Equation (4) does not need any value for the bandgap energy. Nevertheless, Equations (1) and (2) and Equation (4) can be connected to the SQ model by setting the quantum efficiency of the solar cell to $Q_e^{\text{PV}}(E) = a(E) = H(E - E_g^{\text{SQ}})$ with the Heaviside function $H(E - E_g^{\text{SQ}}) = 1$ for $E \geq E_g^{\text{SQ}}$ and $H(E - E_g^{\text{SQ}}) = 0$ otherwise. In the following, we will use the superscript SQ for quantities derived within the SQ model, e.g., $V_{\text{oc}}^{\text{SQ}}$ for the open-circuit voltage in the SQ limit.

According to detailed balance, the voltage loss between the radiative limit $V_{\text{oc}}^{\text{rad}}$ of the open-circuit voltage and the actual open-circuit voltage V_{oc} should scale with the logarithm of the external luminescence quantum efficiency Q_e^{lum} via^[24,25]

$$\Delta V_{\text{oc}}^{\text{nrad}} = V_{\text{oc}}^{\text{rad}} - V_{\text{oc}} = \frac{-kT}{q} \ln\{Q_e^{\text{lum}}\} > 0 \quad (5)$$

The external luminescence quantum efficiency, sometimes also denoted as external radiative efficiency^[15,26] or LED quantum efficiency^[24,27] is an important and well-defined figure of merit^[19] that is suitable to compare the recombination limitation of different solar cell technologies among each other.^[4,15,20,26]

The direct measurement of the (photovoltaic) external quantum efficiency Q_e^{EQE} of the solar cell, typically performed using a grating monochromator setup, usually does not cover the entire energy range of interest for the calculation of J_0^{rad} since its dynamic range is not sufficiently large to cover the relevant absorption edge. Since for the calculation of the saturation-current density, a multiplication of the quantum efficiency with the blackbody spectrum takes place (Equation (2)), especially the values of the quantum efficiency at low energies are weighted exponentially more and hence are decisive for the resulting value of J_0^{rad} . Therefore, a precise determination of J_0^{rad} requires an extended quantum efficiency dataset, which additionally contains values at low energies. This extended quantum efficiency can be obtained by applying the optoelectronic reciprocity theorem, which connects the electroluminescent emission of a solar cell with its photovoltaic quantum efficiency^[24] and the voltage V via

$$\phi_{\text{EL}}(E) = Q_e^{\text{PV}}(E) \phi_{\text{bb}}(E) \left\{ \exp\left(\frac{qV}{kT}\right) - 1 \right\} \quad (6)$$

This relation enables the conversion of one parameter into the other. Thus, it is possible to use a measurement of the electroluminescence (EL) spectrum $\phi_{\text{EL}}(E)$ to obtain the missing values for the quantum efficiency of the solar cell for the low energy range and to combine them with the directly measured quantum efficiency $Q_e^{\text{EQE}}(E)$.^[18,28] The extension of the photovoltaic quantum efficiency using electroluminescence data via Equation (6) has previously been used for perovskite solar cells^[29,30] and other solution processable semiconductors.^[31,32] However, in many cases only the bandgap or the bandgap derived $V_{\text{oc}}^{\text{SQ}}$ is used.^[12–14,33–35] Part of the reason for the absence of $V_{\text{oc}}^{\text{rad}}$ may be that the luminescence spectrum has to be measured with a setup that is at least calibrated for spectral shape (but not necessarily for absolute intensity).

With this analysis we obtain two loss terms for the actual open-circuit voltage V_{oc} , namely, the difference $\Delta V_{\text{oc}}^{\text{rad}} = V_{\text{oc}}^{\text{SQ}}(E_g) - V_{\text{oc}}^{\text{rad}}$ between the SQ value (for the idealized step-function like quantum efficiency) and the radiative value corresponding to the actually measured $Q_e^{\text{EQE}}(E)$ as well as the nonradiative loss term $\Delta V_{\text{oc}}^{\text{nrad}} = V_{\text{oc}}^{\text{rad}} - V_{\text{oc}}$.^[4] Thus, we may write the overall difference

$$\Delta V_{\text{oc}} = V_{\text{oc}}^{\text{SQ}}(E_g) - V_{\text{oc}} = \Delta V_{\text{oc}}^{\text{rad}}(E_g) + \Delta V_{\text{oc}}^{\text{nrad}} \quad (7)$$

between $V_{\text{oc}}^{\text{SQ}}$ and V_{oc} as the sum of those two loss terms. It is obvious from Equation (7) that the actual value of ΔV_{oc} depends on the choice of the bandgap energy E_g . For instance, a method for the determination of E_g that leads to lower values compared to another method would also yield a lower estimate for the open-circuit voltage loss.

3. Definitions of Bandgap Used in the Literature

Publications in the research field of perovskite solar cells currently use a variety of different bandgap definitions for solar cell devices, which are moreover based on different approaches and measurement methods.^[12–14,17,33–36] The bandgap, which is determined by one of these different methods, is often used to calculate the reference open-circuit voltage $V_{\text{oc}}^{\text{SQ}}(E_g)$ which is then compared to the actual value V_{oc} in order to rate the loss ΔV_{oc} (Equation (7)) with the intention of comparing different solar cell types in order to rank the results from a variety of research groups.^[13,17,37]

In this section we will explain and compare different methods for defining the bandgap of a solar cell, commonly used in literature. By applying these methods to an exemplary dataset, we will show that, depending on the chosen method, the calculated value for the bandgap varies substantially. Subsequently, we calculate the open-circuit voltages in the SQ limit for the different bandgap definitions, in order to demonstrate that the corresponding difference propagates further and affects the V_{oc} limit even more in relative terms.

The first method we are going to introduce is the Tauc method,^[38,39] which is, in contrast to most of the other methods, based on the use of absorption coefficient data. The absorption coefficient α is a material property, which results from the characteristic energy-band structure, so that for an ideal, defect-free semiconductor with a direct bandgap the absorption coefficient

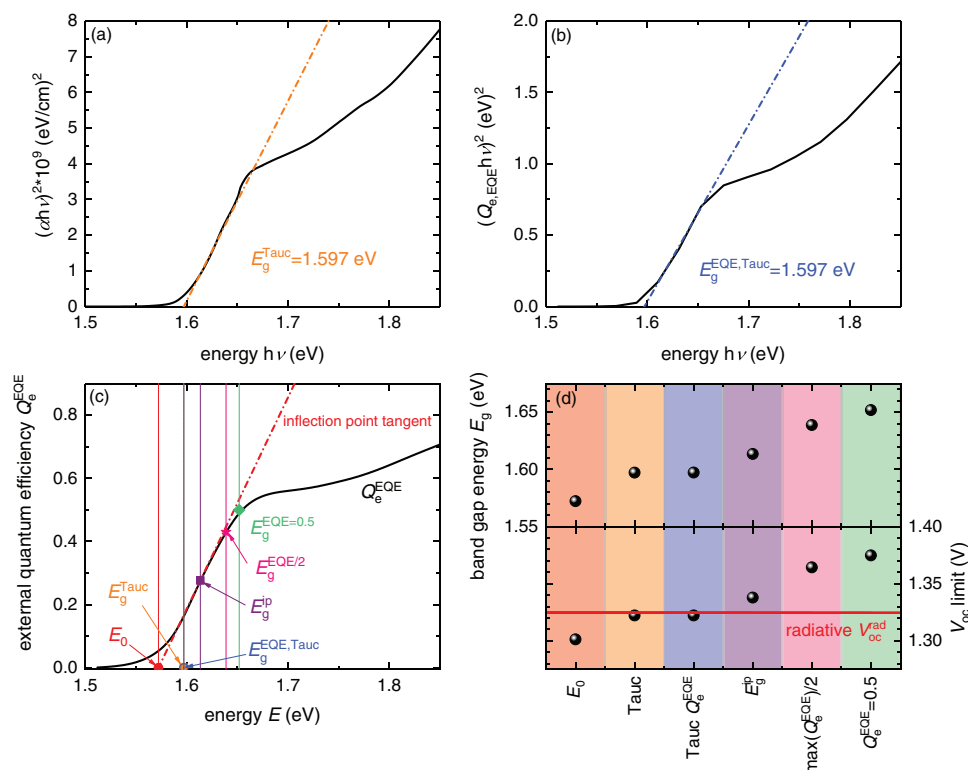


Figure 1. a–c) Determination of the bandgap energy for an exemplary dataset^[17] (optical data of MAPI and quantum efficiency data of a respective MAPI solar cell) using different methods applied in literature. a) The Tauc plot method (orange), which extracts the bandgap E_g^{Tauc} from absorption coefficient data and b) the Tauc plot method, which is adapted to quantum efficiency data yields in $E_g^{\text{Tauc, EQE}}$ (blue). c) Several methods which use characteristic points of the external quantum efficiency Q_e^{EQE} of the solar cell to determine a bandgap energy. These respective characteristic energy values stated in (c), are the inflection point E_g^{IP} of the Q_e^{EQE} (purple), the x-axis intercept of the inflection point tangent E_0 (red), the energy $E_g^{\text{EQE}/2}$ for which the Q_e^{EQE} reaches half of its maximum value (pink), or the energy $E_g^{\text{EQE}=0.5}$ for which the Q_e^{EQE} reaches 50% (green). d) Comparison of the resulting bandgap energy values for all presented methods revealing a huge deviation. e) In addition, we calculate the limit of the open-circuit voltage for respective bandgaps in the SQ limit and the radiative limit V_{oc}^{rad} .

is related to the band gap energy via $\alpha \propto \sqrt{h\nu - E_g}/h\nu$,^[40] with the frequency ν . Based on this theoretical shape of the absorption coefficient α , mathematical transformation yields

$$(\alpha h\nu)^2 \propto h\nu - E_g \quad (8)$$

For the Tauc method, $(\alpha h\nu)^2$ is then plotted as a function of energy $h\nu$ and the linear region is fitted, so that the bandgap results from an extrapolation of this linear fit to the x-axis^[38,39] as shown in Figure 1a. The course of the data also illustrates that the actual shape of the absorption coefficient of metal-halide perovskites, in this case of MAPI ($\text{CH}_3\text{NH}_3\text{PbI}_3$), does not fit well with the theoretical one.^[41–43] Inherent structural disorder of a material creates absorption tail states toward lower photon energies, which become apparent as an exponential tail in the absorption coefficient, called Urbach tail.^[44,45] The slope of this exponential part varies with the degree of disorder and is characterized by the Urbach energy E_{Urbach} .^[20,45,46] Additionally, to the mismatch between theoretical and measured shape of the absorption coefficients, the bandgap determined by the Tauc method represents an internal property of the photovoltaic material and is not an external property of the solar cell device, as it is assumed in the SQ limit.

However, the application of the Tauc method can be extended and applied to external quantum efficiency Q_e^{EQE} data if we assume that for efficient charge collection quantum efficiency equals absorbance and the absorbance can be described by a simple Lambert-Beer model. Under these assumptions, the Q_e^{EQE} and the absorption coefficient should be proportional to each other for low photon energies and absorption coefficients. The Taylor expansion of the absorbance $\alpha(E)d \rightarrow 0$ yields

$$Q_e^{\text{EQE}} \propto a(E) = 1 - \exp(-\alpha(E)d) \approx \alpha(E)d \quad (9)$$

Figure 1b shows the result of the Tauc method, being applied to quantum efficiency Q_e^{EQE} . Both datasets in Figure 1a,b yield similar values for the bandgap. Note that the values for $E_g^{\text{Tauc, EQE}}$ and E_g^{Tauc} do not necessarily agree with each other, as we will see later during the discussion of literature data.

Other common methods, which are applied to determine the bandgap of a solar cells, use different characteristic points of quantum efficiency Q_e^{EQE} and thereby indicate an external property of the solar cell device. An overview over these characteristic points is shown in Figure 1c for the exemplary dataset. The energy $E_g^{\text{EQE}/2}$ at which the quantum efficiency Q_e^{EQE} reaches half its maximum value or the energy $E_g^{\text{EQE}=0.5}$ at which

the quantum efficiency is 50% are for instance such characteristic points.^[12] Another convention, henceforth referred to as the E_0 method, defines the energy E_0 at the x -axis intercept of the inflection-point tangent as bandgap.^[33,34,47] A related approach is to use the inflection point E_g^{ip} itself,^[12] which has the advantage that a constant inflection point often leads to small differences in J_{sc} for differently sharp absorption onset because gains and losses are roughly compensating. The inflection point for fairly sharp and symmetric onsets as present in halide perovskites is also identical to the concept of the photovoltaic bandgap introduced in ref. [4] and used in recent overviews of photovoltaic technologies (see Figure S1 in the Supporting Information).^[15,48]

The comparison of all the different bandgap energies, which we obtained by analyzing absorption and quantum efficiency data for an exemplary dataset is summarized in Figure 1d and reveals how decisive the choice of the method is for the determined bandgap value. The bandgap differs in this example roughly 80 meV, with the E_0 method leading to a rather small bandgap value, the use of the inflection points yields a medium value and characteristic points, such as the half maximum of the Q_e^{EQE} , yield larger bandgap energies. Subsequently, we calculate the SQ limit for the different bandgap definitions. The corresponding limit of the open-circuit voltage is plotted in Figure 1e. This overview of different $V_{\text{oc}}^{\text{SQ}}$ s shows a similar spread as the bandgap energies, i.e., roughly 80 mV. Moreover, it has a huge impact, which V_{oc} limit is used to state the non-radiative voltage losses and compared to the actually measured open-circuit voltage, in this particular case 1.26 V. Depending on the method, the losses are ≈ 40 mV in the best case (i.e., for the definition leading to the smallest bandgap) and up to 115 mV for the most conservative (i.e., highest) estimate of bandgap. Hence, if one were to estimate Q_e^{lum} from the different voltage losses mentioned above, the variation in Q_e^{lum} would range from 1% (for 115 mV) to 50% (for 40 mV). Thus, the different bandgap definitions lead to a spread in bandgap energies that is of a similar magnitude as the energy losses under investigation, thereby rendering comparisons between different solar cells meaningless. As a result, the research community should agree on one suitable, consistent method of referencing to enable a comprehensive, simple, fair and meaningful comparison of nonradiative voltage losses and to allow a rating of the measured V_{oc} values among various perovskite compositions.

In the following section, we make a proposal for such a standardized method to state the V_{oc} limit and voltage losses, which we believe is meaningful and at the same time convenient and easy to apply. Our approach is an approximated version of the radiative limit that only requires a single measurement of the external quantum efficiency of the solar cell for its calculation. Usually, as explained in Section 1, external quantum efficiency $Q_e^{\text{EQE}}(E)$ and EL emission data $\phi_{\text{EL}}(E)$ are both needed and combined by using Equation (6) to precisely determine the radiative open-circuit voltage $V_{\text{oc}}^{\text{rad}}$. **Figure 2a** shows respective EQE and EL measurements for our exemplary MAPI solar cell, the converted parameters obtained by using the reciprocity relation and the extended quantum efficiency $Q_e^{\text{PV}}(E)$, which covers the entire energy range of interest. Using Equation (1)–(4), gives the radiative limit for the open-circuit voltage of 1.324 V. From

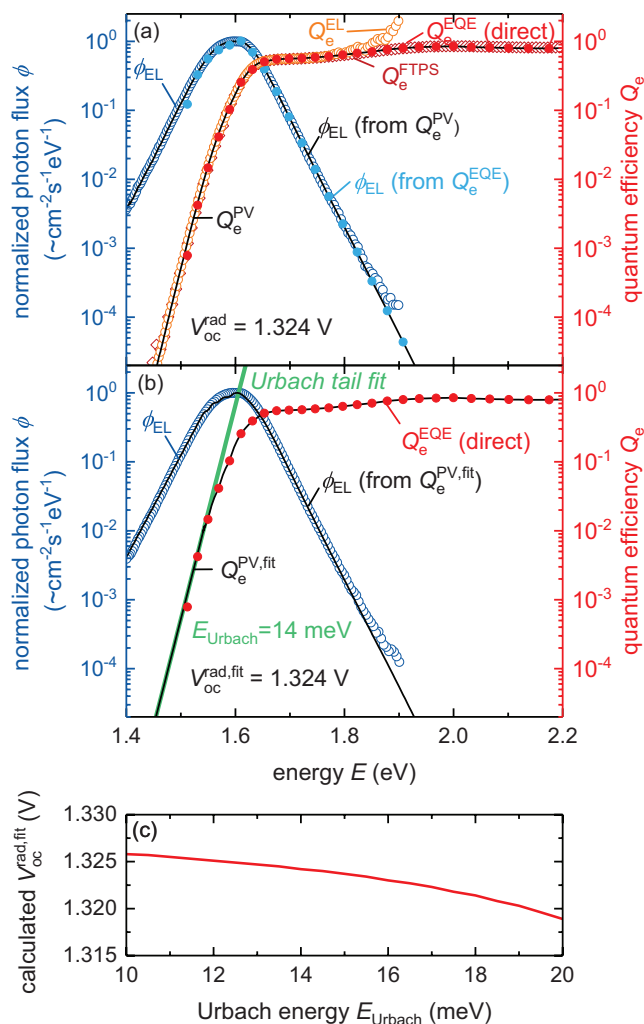


Figure 2. a) Electroluminescence spectrum $\phi_{\text{EL}}(E)$ (dark blue) and quantum efficiency $Q_e^{\text{EQE}}(E)$ from (EQE (red) and $Q_e^{\text{FTPS}}(E)$ from Fourier transform photocurrent spectroscopy (FTPS) (dark red)) of the exemplary MAPI cell from Figure 1, converted via reciprocity relation in one another (light blue and orange), and finally combined to an extended $Q_e^{\text{PV}}(E)$, which is then used to calculate the radiative open-circuit voltage $V_{\text{oc}}^{\text{rad}}$. From this calculation results a thermodynamic limit for the open-circuit voltage of 1.324 V for the respective device. Reproduced with permission.^[17] Copyright 2019, American Chemical Society. b) Calculation of the radiative limit from measured quantum efficiency $Q_e^{\text{EQE}}(E)$ data, to which a fit of the Urbach tail was attached to obtain $Q_e^{\text{PV,fit}}(E)$. An Urbach energy of 14 meV fits best to the exponential decay and yields the same V_{oc} limit of 1.324 V. c) The radiative open-circuit voltage $V_{\text{oc}}^{\text{rad,fit}}$ as a function of Urbach energy E_{Urbach} .

the course of the overall $Q_e^{\text{PV}}(E)$ at the band edge, it becomes apparent that it is a sharp, exponential Urbach tail with a slope being already apparent in the measured $Q_e^{\text{EQE}}(E)$ data and no other characteristics occur. Therefore, the absorption edge will be dominated by the factor

$$\alpha(E) \propto C \cdot \exp(E/E_{\text{Urbach}}) \quad (10)$$

with the Urbach energy E_{Urbach} and C a prefactor. For metal-halide perovskites the room-temperature Urbach energy is usually

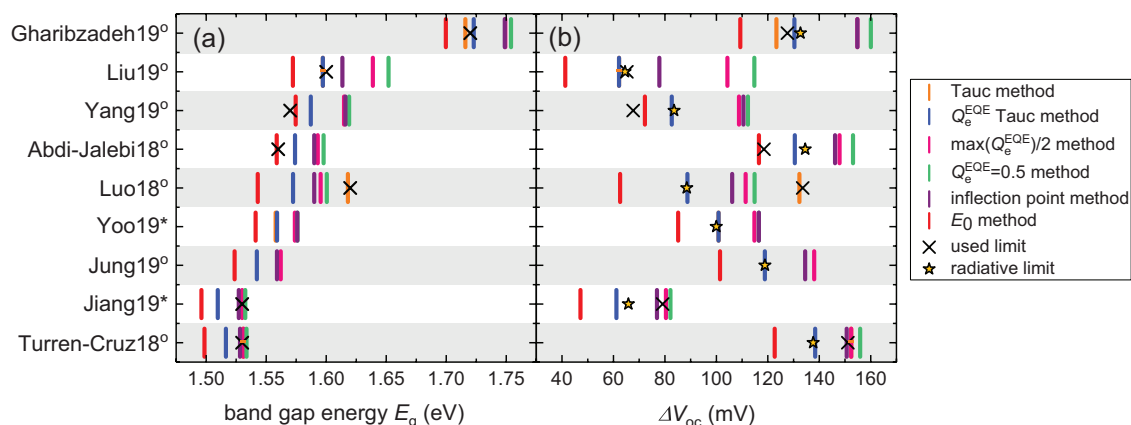


Figure 3. Comparison of solar cells from literature (°: champion devices, *: certified) with exceptionally high $V_{oc,S}$,^[12–14,17,33–36,47] which were evaluated with the different methods for bandgap determination introduced in Section 3. a) The different values of the bandgap energy. b) The voltage losses, calculated by subtracting the reported V_{oc} from the SQ limit of the open-circuit voltage for the bandgap values resulting from each method. In addition, losses with regard to an approximation of the radiative open-circuit voltage (radiative limit) are stated, which were calculated by combining the measured quantum efficiency data from the respective publications and a fit of the Urbach tail to an extended quantum efficiency. Moreover, we quote for each solar cell record the voltage loss as specified in the corresponding publication (marked with an “X”). Since the perovskite composition and thereby the bandgap range change, these stated ΔV_{oc} values are not comparable, because different methods were used for the analysis.

around 15 meV.^[10,35] Utilizing this simple behavior opens up the possibility of generating the missing quantum efficiency values at low energies through a fit of an Urbach tail. We apply this idea to our exemplary $Q_e^{EQE}(E)$ dataset and obtain for the radiative open-circuit-voltage $V_{oc}^{rad,fit}$ from the fit a value that is good agreement with V_{oc}^{rad} . The fitted Urbach tail and the resulting overall $Q_e^{PV,fit}(E)$ are shown in Figure 2b (detailed discussion in the Supporting Information).

Furthermore, we evaluated this approximation of the radiative limit for different Urbach energies to point out that the accuracy of the slope of the Urbach tails has no significant influence on the determined $V_{oc}^{rad,fit}$ value. As shown in Figure 2c, the $V_{oc}^{rad,fit}$ deviates by a few millivolts if E_{Urbach} is varied by 10 meV, which is negligible compared to the deviation of 80 mV that could occur when using different bandgap definitions and not only one consistent method of referencing (Figure 1e). The quality of the fit is therefore not decisive for the determination of $V_{oc}^{rad,fit}$. In summary, we conclude that the approximate determination of the radiative limit from a combination of measured $Q_e^{EQE}(E)$ and Urbach tail fit is suitable method to determine the limit for the open-circuit voltage, easily done, but still precisely enough (MATLAB script available). Thus, as long as a measurement of the external photovoltaic quantum efficiency is available for the specific device the determination of the radiative open-circuit voltage is possible.

4. Meta-Analysis of Literature Data

The last section has provided an overview of various methods used in the literature to determine the bandgap, its corresponding SQ limit of the open-circuit voltage and the radiative limit calculated for an exemplary dataset. In this section, we apply all these introduced methods to external quantum efficiency data and if available to absorption data of previously published perovskite solar cells with exceptionally high open-circuit

voltages.^[12–14,17,33–36,47] In Figure 3a) the different values of bandgap energy are plotted and in Figure 3b) we compare the corresponding voltage losses ΔV_{oc} , so the difference between the values of the calculated V_{oc} limits and the stated V_{oc} .

Just as for the exemplary dataset in Figure 1, the resulting values for E_g and ΔV_{oc} are quite different and widespread depending on the applied method. The E_0 method (red) leads in each case to rather small bandgap values and thus to very small voltages losses, so it is a very optimistic calculation, which always yields smaller values than the radiative limit (yellow star). All other methods are not so clearly arranged and do not always show the same trend for all considered high-performance devices. Values for the bandgap energy such as $E_g^{EQE=0.5}$ can be rather different, since the layer thickness, which changes the transparency, and optical interference effects in these layer stacks, modify the shape of the quantum efficiency.

In addition to our calculated values of the bandgap energies and the voltage losses, Figure 3 also shows the values that are actually stated in the respective publications (used limit). Since various perovskite compositions and the whole range of different methods are used, some results are rather optimistic in their assessment of voltage losses (Yang et al.^[33] or Abdi-Jalebi et al.^[34]) while others are quite conservative (Jiang et al.^[12] or Turren-Cruz et al.^[14]). Comparisons of values between different papers is hence either misleading or only possible if the differences are huge, i.e., much larger than the bandgap range caused by the different bandgap definitions.

5. Figures of Merit for Perovskite Solar Cells

In the following, we therefore use for the first time an identical way of referencing to compare all devices and to enable an unbiased, comprehensive comparison, which reveals the respective device limitations. Figure 4 gives an overview of the

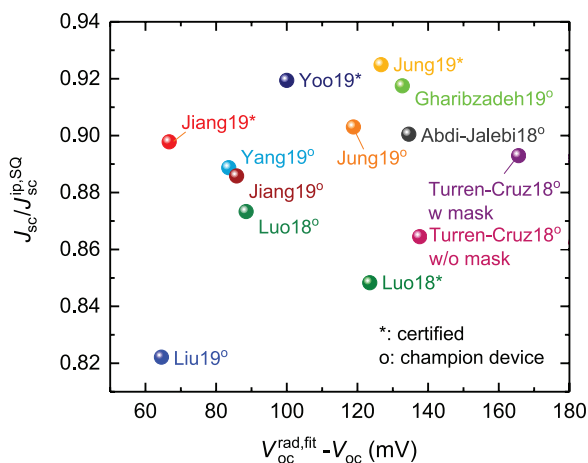


Figure 4. Comparison of the limitations of the different record perovskite solar cells from literature,^[12–14,17,33–36,47] all being analyzed by using one consistent method to determine the bandgap and the limit of the open-circuit voltage. In this way, the losses are comparable with each other and an unbiased comparison is possible. The performance with regard to the short-circuit current density is indicated by the ratio of experimental J_{sc} compared to the Shockley–Queisser (SQ) limit. For the nonradiative voltage losses we subtract the measured open-circuit voltage from the radiative limit $V_{oc}^{rad,fit}$.

resulting losses in J_{sc} and V_{oc} for the high-performance solar cells studied in our meta-analysis. As a figure of merit (FoM) for the limitations due to nonradiative voltage losses the difference between their respective radiative limits, which were calculated from the extended quantum efficiencies $Q_e^{PV,fit}(E)$ and the reported open-circuit voltages, is used. Moreover, we have a look at the reported short-circuit current densities J_{sc} , which mainly indicates how good the respective devices absorb light, and consider them in relation to the one in the SQ limit J_{sc}^{SQ} (inflection point is used as bandgap). The performance of the device from Jiang et al.^[12] stands out, because it has both extremely small losses in short-circuit current density and in open-circuit voltage, and the voltage losses were rated too pessimistic in the actual publication. In addition, it is curious to note that the solar cell published by Gharibzadeh et al.^[13] was advertised in the title of the paper because of its high V_{oc} , despite the fact that if bandgap and radiative V_{oc} are considered, the cell actually excels in J_{sc} . Only an identical way of referencing perovskite solar cells with varying compositions helps to explicitly highlight these peculiarities or limitations, which otherwise remain unnoticed. In addition, comparison of losses as done in Figure 4 is important because it allows us to better identify which aspects to target for further efficiency improvements. For instance, work on surface passivation would be highly valuable if open-circuit voltage losses are substantial but would be less relevant if the losses appear mainly in J_{sc} .

The use of a consistent definition of bandgap (via the inflection point method) also allows us to make a historical analysis of efficiencies, normalized efficiencies and bandgaps as shown in Figure 5 for the material class of lead-halide perovskites. While not all efficiency records over the years were published in a scientific journal, it is at least possible to trace the key

developments during the years based on published data that we can analyze in the same way as discussed above. Figure 5a shows the development in efficiency starting with 15% MAPbI₃ solar cells in 2013 and ending with current >23% efficiency devices based on FA_{0.92}MA_{0.08}PbI₃. As shown in Figure 5b, part of the development toward higher efficiencies was driven by a reduction of the bandgap by adding different amounts of formamidinium (FA) and sometimes Cs to double or triple cation blends. Due to the different amounts of Br added to the initially purely I-based perovskites, the bandgap continuously varied. Figure 5c shows the development of the efficiency normalized to the SQ efficiency for the given bandgap (using the inflection point to calculate the SQ efficiency). While good MAPI cells in 2013 were still below 50% of the bandgap specific SQ limit, values exceeded already 72% in 2016 and have risen only moderately since then (to ≈73%). Most of the efficiency gains relative to the quadruple cation perovskites presented by Saliba et al.^[49] are mainly due to a reduction in bandgap. It is clear that while this is a valid path to go for increasing single junction efficiencies, any efforts toward tandem solar cells benefit from either substantially lower (1.25 eV or lower)^[50] or slightly higher bandgaps (≈1.65–1.85 eV).^[51,52]

Figure 5d shows the development of nonradiative voltage losses ΔV_{oc}^{nrad} as a function of time for the same set of cells. The voltage losses decrease continuously until again about 2016, where the data published in ref. [49] already achieves a level of ΔV_{oc}^{nrad} typical also for later record cells. Note that we used the highest efficiency cell in ref. [49] and not the highest V_{oc} cell for this comparison, which implies that even lower voltage losses were possible with this layer stack. During recent years, among the highest efficiency cells, only the data in the paper by Jiang et al.^[12] stands out in terms of extremely low ΔV_{oc}^{nrad} as previously mentioned.

Recently, we have shown how to break down the losses in a solar cell into several factors, each of which can be considered as a figure of merit highlighting different physical loss mechanisms and in consequence different optimization strategies.^[19] The normalized efficiency used before in Figure 5c can be expressed as

$$\frac{\eta_{real}}{\eta_{SQ}} = F_{sc} \frac{V_{oc}^{real} FF_0(V_{oc}^{real})}{V_{oc}^{SQ} FF_0(V_{oc}^{SQ})} F_{FF}^{res} \quad (11)$$

where $F_{sc} = J_{sc}/J_{sc}^{SQ}$ (yellow in Figure 6). Note that the maximum possible fill factor (FF) of a solar cell is a function of the open-circuit voltage.^[61,62] The rationale behind that effect is that the difference between the voltage V_{mpp} at the maximum power point and the V_{oc} is relatively constant, which implies that the ratio V_{mpp}/V_{oc} which controls the value of the ideal fill factor is not constant but a function of V_{oc} . Hence, the fill factor losses in Equation (11) are split in two parts, one ($FF_0(V_{oc}^{real})/FF_0(V_{oc}^{SQ})$) (purple in Figure 6) dealing with the fill factor loss due to the loss in open-circuit voltage and a second one called F_{FF}^{res} taking into account additional losses which are mainly resistive in nature. Also the losses in V_{oc} are split up in two parts, namely, into losses due to the discrepancy between the actual shape quantum efficiency and the ideal step-function assumed in the SQ limit, which is described by the ratio of $V_{oc}^{rad,fit}/V_{oc}^{SQ}$

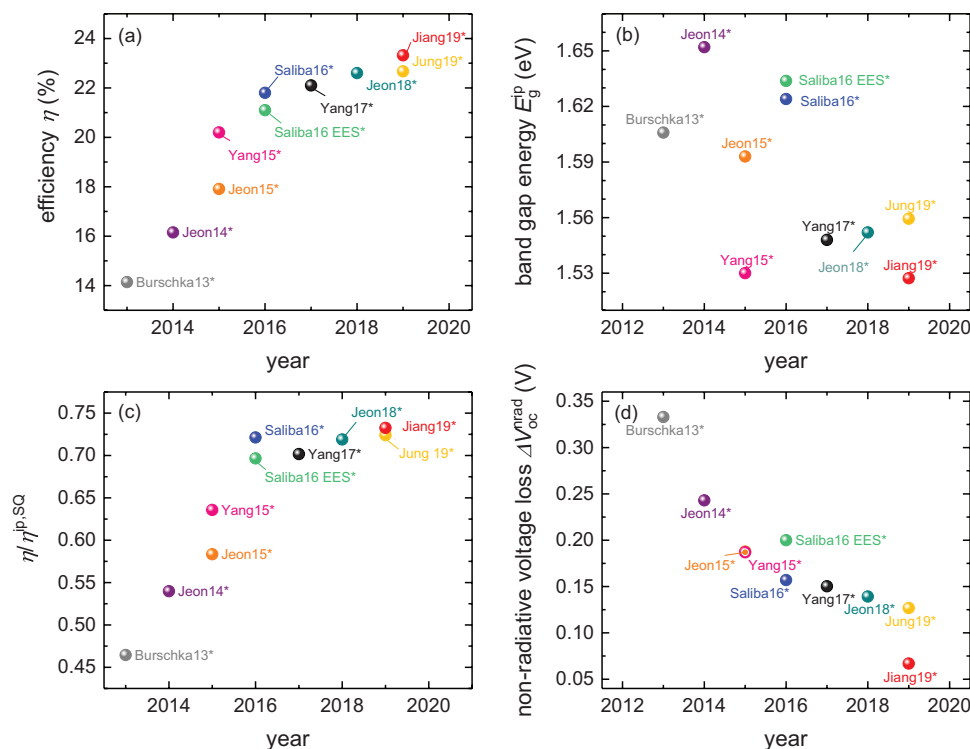


Figure 5. Overview over the development of certified record device characteristics^[12,36,49,53–59] over time, most of them are stated in the NREL solar cell efficiency tables.^[60] a) The progress of record efficiency is shown. b) The respective bandgap energy E_g^{ip} (inflection point energy of the external quantum efficiency) and c) the ratio of efficiency to the one in SQ limit calculated for E_g^{ip} are shown. d) Trend of the nonradiative losses in open-circuit voltage $\Delta V_{\text{oc}}^{\text{rad}}$ over time.

(blue in Figure 6) and losses due to nonradiative recombination $V_{\text{oc}}^{\text{real}}/V_{\text{oc}}^{\text{rad,fit}}$ (green in Figure 6). Moreover, nonradiative losses always reduce the limit of the fill factor, because the FF is linked to the actual open-circuit voltage of the device.^[61] Respective losses in the FF are represented by $FF_0(V_{\text{oc}}^{\text{real}})/FF_0(V_{\text{oc}}^{\text{SQ}})$

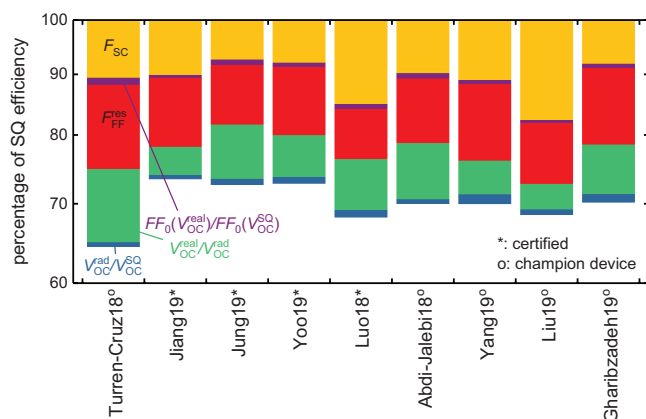


Figure 6. Visualization of potential improvement of top-performing metal-halide perovskite solar cells from literature, based on their bandgaps, relative to the ideal, SQ-case, using partitioning of the efficiency losses, according to ref. [19]. A detailed discussion of these different figures of merit (FoMs) is available in the Supporting Information of ref. [19]. As a reference bandgap, we use the photovoltaic bandgap E_g^{ip} extracted from solar cell quantum efficiency data.

(purple). Additionally, resistive losses $F_{\text{FF}}^{\text{res}}$, stated in red in Figure 6, reduce the fill factor. A detailed description and discussion of all FoMs is available in ref. [19].

Figure 6 compares the different loss terms in Equation (11) among the range of recent perovskite solar cells already discussed in Figure 3 and 4. Note that the y-axis representing the normalized efficiency is a logarithmic axis, implying that the order of the loss factors can be exchanged without changing the relative size of the boxes which would not be the case with a linear axis. A nearly identical plot for record devices from other photovoltaic technologies is presented in the supporting information of ref. [19].

A lot of effort has already been invested in minimizing non-radiative recombination explaining that in the case of high-performance devices, the green bar is no longer the largest in terms of area. Rather, Figure 6 reveals that resistive losses, reducing the fill factor (red), make up the largest share for almost all perovskite solar cells and are the limiting factor. Thus, the comparatively rarely discussed resistive losses^[63] stand out as providing the highest potential for further improvement and are notably substantially higher than in more mature technologies such as GaAs, Si or Cu(In,Ga)Se₂.^[19]

6. Conclusions

The key statement of the paper is that considering the different definitions of bandgaps in lead-halide perov-

skites is important for fair comparisons of remarkably high performance and in particular for high open-circuit voltages. This is due to the fact that any claim of high performance is implicitly or explicitly made relative to some reference that serves to define one's expectations. This reference has in the past mostly been the so-called Shockley–Queisser limit for a specific bandgap that was determined in different ways from paper to paper. Here we suggest a slightly different procedure: For referencing high open-circuit voltages, the bandgap is not necessary and can easily be replaced by the more precise determination of the so-called radiative limit of V_{oc} , which can be calculated using the external quantum efficiency of the solar cell. For typical dynamic ranges used for quantum efficiency measurements small parts of the quantum efficiency data have to be extrapolated which is however easily done by assuming an exponential band tail. This assumption works well for lead-halide perovskites, because a room-temperature Urbach tail of 13–15 meV is usually found in this material class.^[44] Accompanying this paper, the reader finds a MATLAB script that allows calculating the radiative V_{oc} based on experimental quantum efficiency data used as input. If efficiency and other device parameters have to be referenced to their Shockley–Queisser limit, the calculation of the latter forces us to determine a bandgap. For this purpose, we propose to use the inflection point of the external quantum efficiency. The Shockley–Queisser model is based on the idea of looking at the external properties of a solar cell and is agnostic to the actual material properties. In this logic, we therefore suggest to use a method to determine the bandgap that is based on externally observable properties such as the external quantum efficiency and that does not require specific assumptions on the properties of the absorber material. The inflection point fulfills these requirements and thereby facilitates comparisons between different material classes (e.g., crystalline and amorphous silicon, organic solar cells).^[4] Finally, the inflection point method reduces the risk of obtaining negative voltage losses $V_{oc}^{SQ} - V_{oc}^{rad}$ due to a smeared out absorption edge and thereby simplifies quantifications of efficiency losses as shown in Figure 6 (for details see Figure S2 and accompanying discussion in the Supporting Information).

A consistent comparison of different perovskite solar cells in terms of their efficiencies, bandgaps and specific loss factors, suggests that while efficiencies are continuously improving, these improvements are for the past three years mostly due to reductions in bandgap and hence a more efficient use of the solar spectrum. However, given that efforts toward multijunction solar cells become increasingly important, the efficiency can no longer be the only figure of merit. Rather, normalized efficiencies for certain bandgap ranges needed for tandem solar cells would be a more suitable metric. Finally, quantitative comparisons of specific loss contributions for state-of-the-art perovskite solar cells suggest that a common shortcoming is the still fairly low fill factor caused most likely by resistive losses and most likely to a certain degree by high ideality factors. Fill factors in excess of 90% are thermodynamically possible for lead-halide perovskite solar cells with typical bandgaps around 1.6 eV,^[64] but typical values for the fill factor are most often in the range of 80% or lower.

Supporting Information

Supporting Information is available from the Wiley Online Library or from the author.

Acknowledgements

L.K., T.K., and U.R. acknowledge the Helmholtz Association for funding via the PEROSEED project. The authors thank Jingbi You (Beijing) for providing the data used in ref. [12].

Conflict of Interest

The authors declare no conflict of interest.

Keywords

bandgap, fill factor losses, nonradiative voltage losses, photovoltaics, radiative limit, recombination, Shockley–Queisser model

Received: August 7, 2019

Revised: October 7, 2019

Published online: November 11, 2019

- [1] T. Markvart, *Phys. Status Solidi A* **2008**, 205, 2752.
- [2] T. Markvart, *Appl. Phys. Lett.* **2007**, 91, 064102.
- [3] L. C. Hirst, N. J. Ekins-Daukes, *Prog. Photovoltaics* **2011**, 19, 286.
- [4] U. Rau, B. Blank, T. C. Müller, T. Kirchartz, *Phys. Rev. Appl.* **2017**, 7, 044016.
- [5] M. Gloeckler, J. Sites, *J. Phys. Chem. Solids* **2005**, 66, 1891.
- [6] G. D. Cody, T. Tiedje, B. Abeles, B. Brooks, Y. Goldstein, *Phys. Rev. Lett.* **1981**, 47, 1480.
- [7] Y. Wang, D. Qian, Y. Cui, H. Zhang, J. Hou, K. Vandewal, T. Kirchartz, F. Gao, *Adv. Energy Mater.* **2018**, 8, 1801352.
- [8] K. Vandewal, J. Benduhn, V. Nikolis, *Sust. Energy Fuels* **2018**, 2, 538.
- [9] V. C. Nikolis, J. Benduhn, F. Holzmueller, F. Piersimoni, M. Lau, O. Zeika, D. Neher, C. Koerner, D. Spoltore, K. Vandewal, *Adv. Energy Mater.* **2017**, 7, 1700855.
- [10] S. De Wolf, J. Holovsky, S.-J. Moon, P. Löper, B. Niesen, M. Ledinsky, F.-J. Haug, J.-H. Yum, C. Ballif, *J. Phys. Chem. Lett.* **2014**, 5, 1035.
- [11] E. Unger, L. Kegelmann, K. Suchan, D. Sörell, L. Korte, S. Albrecht, *J. Mater. Chem. A* **2017**, 5, 11401.
- [12] Q. Jiang, Y. Zhao, X. Zhang, X. Yang, Y. Chen, Z. Chu, Q. Ye, X. Li, Z. Yin, J. You, *Nat. Photonics* **2019**, 13, 460.
- [13] S. Gharibzadeh, B. Abdollahi Nejand, M. Jakoby, T. Abzieher, D. Hauschild, S. Moghadamzadeh, J. A. Schwenzer, P. Brenner, R. Schmager, A. A. Haghighirad, L. Weinhardt, U. Lemmer, B. S. Richards, I. A. Howard, U. W. Paetzold, *Adv. Energy Mater.* **2019**, 9, 1803699.
- [14] S.-H. Turren-Cruz, A. Hagfeldt, M. Saliba, *Science* **2018**, 362, 449.
- [15] M. A. Green, A. W. Ho-Baillie, *ACS Energy Lett.* **2019**, 4, 1639.
- [16] W. Shockley, H. J. Queisser, *J. Appl. Phys.* **1961**, 32, 510.
- [17] Z. Liu, L. Krückemeier, B. Krogmeier, B. Klingebiel, J. A. Márquez, S. Levchenko, S. Öz, S. Mathur, U. Rau, T. Unold, T. Kirchartz, *ACS Energy Lett.* **2019**, 4, 110.
- [18] T. Kirchartz, U. Rau, M. Kurth, J. Mattheis, J. Werner, *Thin Solid Films* **2007**, 515, 6238.

- [19] J.-F. Guillemoles, T. Kirchartz, D. Cahen, U. Rau, *Nat. Photonics* **2019**, 13, 501.
- [20] J. Yao, T. Kirchartz, M. S. Vezie, M. A. Faist, W. Gong, Z. He, H. Wu, J. Troughton, T. Watson, D. Bryant, J. Nelson, *Phys. Rev. Appl.* **2015**, 4, 014020.
- [21] T. Tiedje, E. Yablonovitch, G. D. Cody, B. G. Brooks, *IEEE Trans. Electron Devices* **1984**, 31, 711.
- [22] U. Rau, J. Werner, *Appl. Phys. Lett.* **2004**, 84, 3735.
- [23] T. Kirchartz, K. Taretto, U. Rau, *J. Phys. Chem. C* **2009**, 113, 17958.
- [24] U. Rau, *Phys. Rev. B* **2007**, 76, 085303.
- [25] R. T. Ross, *J. Chem. Phys.* **1967**, 46, 4590.
- [26] M. A. Green, *Prog. Photovoltaics* **2012**, 20, 472.
- [27] T. Kirchartz, U. Rau, *Phys. Status Solidi A* **2008**, 205, 2737.
- [28] T. Kirchartz, U. Rau, *J. Appl. Phys.* **2007**, 102, 104510.
- [29] K. Tvingstedt, O. Malinkiewicz, A. Baumann, C. Deibel, H. J. Snaith, V. Dyakonov, H. J. Bolink, *Sci. Rep.* **2015**, 4, 6071.
- [30] W. Tress, N. Marinova, O. Inganäs, M. K. Nazeeruddin, S. M. Zakeeruddin, M. Graetzel, *Adv. Energy Mater.* **2015**, 5, 1400812.
- [31] K. Vandewal, K. Tvingstedt, A. Gadisa, O. Inganäs, J. V. Manca, *Nat. Mater.* **2009**, 8, 904.
- [32] K. Vandewal, S. Albrecht, E. T. Hoke, K. R. Graham, J. Widmer, J. D. Douglas, M. Schubert, W. R. Mateker, J. T. Bloking, G. F. Burkhard, A. Sellinger, J. M. J. Fréchet, A. Amassian, M. K. Riede, M. D. McGehee, D. Neher, A. Salleo, *Nat. Mater.* **2014**, 13, 63.
- [33] S. Yang, J. Dai, Z. Yu, Y. Shao, Y. Zhou, X. Xiao, X. C. Zeng, J. Huang, *J. Am. Chem. Soc.* **2019**, 141, 5781.
- [34] M. Abdi-Jalebi, Z. Andaji-Garmaroudi, S. Cacovich, C. Stavrakas, B. Philippe, J. M. Richter, M. Alsari, E. P. Booker, E. M. Hutter, A. J. Pearson, S. Lilliu, T. J. Savenije, H. Rensmo, G. Divitini, C. Ducati, R. H. Friend, S. D. Stranks, *Nature* **2018**, 555, 497.
- [35] D. Luo, W. Yang, Z. Wang, A. Sadhanala, Q. Hu, R. Su, R. Shivanna, G. F. Trindade, J. F. Watts, Z. Xu, T. Liu, K. Chen, F. Ye, P. Wu, L. Zhao, J. Wu, Y. Tu, Y. Zhang, X. Yang, W. Zhang, R. H. Friend, Q. Gong, H. J. Snaith, R. Zhu, *Science* **2018**, 360, 1442.
- [36] E. H. Jung, N. J. Jeon, E. Y. Park, C. S. Moon, T. J. Shin, T.-Y. Yang, J. H. Noh, J. Seo, *Nature* **2019**, 567, 511.
- [37] I. L. Braly, D. W. deQuilettes, L. M. Pazos-Outon, S. Burke, M. E. Ziffer, D. S. Ginger, H. W. Hillhouse, *Nat. Photonics* **2018**, 12, 355.
- [38] J. Tauc, *Mater. Res. Bull.* **1968**, 3, 37.
- [39] J. Tauc, *Amorphous and Liquid Semiconductors*, Springer, Boston, MA, **1974**, p. 159.
- [40] B. K. Ridley, *Quantum Processes in Semiconductors*, Oxford University Press, New York, NY **2013**, p. 168.
- [41] X. Chen, H. Lu, Y. Yang, M. C. Beard, *J. Phys. Chem. Lett.* **2018**, 9, 2595.
- [42] T. Wang, B. Daiber, J. M. Frost, S. A. Mann, E. C. Garnett, A. Walsh, B. Ehrler, *Energy Environ. Sci.* **2017**, 10, 509.
- [43] T. Kirchartz, U. Rau, *J. Phys. Chem. Lett.* **2017**, 8, 1265.
- [44] M. Ledinsky, T. Schönfeldová, J. Holovsky, E. Aydin, Z. Hájková, L. Landová, N. Neyková, A. Fejfar, S. De Wolf, *J. Phys. Chem. Lett.* **2019**, 10, 1368.
- [45] F. Urbach, *Phys. Rev.* **1953**, 92, 1324.
- [46] S. John, C. Soukoulis, M. H. Cohen, E. Economou, *Phys. Rev. Lett.* **1986**, 57, 1777.
- [47] J. J. Yoo, S. Wieghold, M. Sponseller, M. Chua, S. N. Bertram, N. T. P. Hartono, J. Tresback, E. Hansen, J.-P. Correa-Baena, V. Bulovic, *Energy Environ. Sci.* **2019**, 12, 2192.
- [48] P. K. Nayak, S. Mahesh, H. J. Snaith, D. Cahen, *Nat. Rev. Mater.* **2019**, 4, 269.
- [49] M. Saliba, T. Matsui, K. Domanski, J.-Y. Seo, A. Ummadisingu, S. M. Zakeeruddin, J.-P. Correa-Baena, W. R. Tress, A. Abate, A. Hagfeldt, *Science* **2016**, 354, 206.
- [50] J. Tong, Z. Song, D. H. Kim, X. Chen, C. Chen, A. F. Palmstrom, P. F. Ndione, M. O. Reese, S. P. Dunfield, O. G. Reid, *Science* **2019**, 364, 475.
- [51] T. Kirchartz, S. Korgitzsch, J. Hüpkens, C. O. R. Quiroz, C. J. Brabec, *ACS Energy Lett.* **2018**, 3, 1861.
- [52] G. E. Eperon, M. T. Hörantner, H. J. Snaith, *Nat. Rev. Chem.* **2017**, 1, 0095.
- [53] J. Burschka, N. Pellet, S.-J. Moon, R. Humphry-Baker, P. Gao, M. K. Nazeeruddin, M. Grätzel, *Nature* **2013**, 499, 316.
- [54] N. J. Jeon, J. H. Noh, Y. C. Kim, W. S. Yang, S. Ryu, S. I. Seok, *Nat. Mater.* **2014**, 13, 897.
- [55] N. J. Jeon, J. H. Noh, W. S. Yang, Y. C. Kim, S. Ryu, J. Seo, S. I. Seok, *Nature* **2015**, 517, 476.
- [56] W. S. Yang, J. H. Noh, N. J. Jeon, Y. C. Kim, S. Ryu, J. Seo, S. I. Seok, *Science* **2015**, 348, 1234.
- [57] M. Saliba, T. Matsui, J.-Y. Seo, K. Domanski, J.-P. Correa-Baena, M. K. Nazeeruddin, S. M. Zakeeruddin, W. Tress, A. Abate, A. Hagfeldt, *Energy Environ. Sci.* **2016**, 9, 1989.
- [58] W. S. Yang, B.-W. Park, E. H. Jung, N. J. Jeon, Y. C. Kim, D. U. Lee, S. S. Shin, J. Seo, E. K. Kim, J. H. Noh, *Science* **2017**, 356, 1376.
- [59] N. J. Jeon, H. Na, E. H. Jung, T.-Y. Yang, Y. G. Lee, G. Kim, H.-W. Shin, S. I. Seok, J. Lee, J. Seo, *Nat. Energy* **2018**, 3, 682.
- [60] M. A. Green, E. D. Dunlop, D. H. Levi, J. Hohl-Ebinger, M. Yoshita, A. W. Y. Ho-Baillie, *Prog. Photovoltaics* **2019**, 27, 565.
- [61] M. A. Green, *Solid-State Electron.* **1981**, 24, 788.
- [62] M. A. Green, *Sol. Cells* **1982**, 7, 337.
- [63] N. Mundhaas, Z. J. Yu, K. A. Bush, H. P. Wang, J. Häusele, S. Kavadiya, M. D. McGehee, Z. C. Holman, *Sol. RRL* **2019**, 3, 1800378.
- [64] T. Kirchartz, *Philos. Trans. R. Soc., A* **2019**, 377, 20180286.